11

Rotational bands – the particle–rotor model

A general frame for the description of rotational states in nuclei was set in the beginning of the fifties by Bohr (1952) and by Bohr and Mottelson (1953). Rotation is a typical example of a collective degree of freedom in nuclei. A collective excitation is characterised by the coherent movement of a large number of nucleons. Thus, an elementary understanding of collective excitations is often achieved from macroscopic models. One example is nuclear fission, which could be considered as some kind of very large amplitude shape vibration. It is then also straightforward to introduce shape vibrations in general as a collective degree of freedom as illustrated in an elementary way in problem 10.2. In a more general context, shape vibrations can be described for example by the variation around the equilibrium value of the $\alpha_{\lambda\mu}$ parameters introduced in chapter 4. The most important and first non-trivial mode corresponds to $\lambda = 2$, quadrupole vibrations.

When describing nuclear quadrupole vibrations in the laboratory system, one has to introduce all the five $\alpha_{2\mu}$ shape parameters. These can, however, be transformed to a body-fixed system where two parameters describe deformations, namely in the ε_2 (or β_2) and the γ degrees of freedom (the γ parameter was introduced in chapter 8). The three additional parameters then describe the orientation of the body-fixed system, e.g. by the three Euler angles. These three parameters thus describe the rotational motion, which is treated in the present chapter and continued in chapter 12. Vibrations, on the other hand, will not be treated here but instead we refer to the literature, e.g. Rowe (1970) and Eisenberg and Greiner (1987).

When it comes to a quantum mechanical description, a further important observation is that one cannot define any collective rotation around a symmetry axis. This is seen from the fact that such a rotation would change only a trivial phase factor in the wave function (for example in the $e^{i\Lambda\varphi}$ part in the single-particle orbitals of a potential with cylindrical symmetry). Such an

unchanged wave function is in contrast to collective rotation. Instead, collective rotation is characterised by small angular momentum contributions from a large number of particles, i.e. the wave functions of these particles change slowly with increasing angular momentum.

What has been said above implies that only deformed nuclei can rotate collectively and, if the nucleus is axially symmetric, the only possible rotation axis is perpendicular to the symmetry axis. For collective rotation, it is then also possible to define *one* moment of inertia, $\mathscr{I}$, leading to the following Hamiltonian

$$H_{\text{rot}} = \frac{\mathbf{R}^2}{2\mathscr{I}}$$

where **R** is the collective angular momentum. For pure collective rotation the total angular momentum (often referred to as the total spin) **I** is equal to **R**. The spectrum then takes the form

$$E_I = \frac{\hbar^2}{2\mathscr{I}} I(I+1).$$

As only deformed nuclei exhibit rotational spectra, it should be possible to determine which nuclei are deformed from the occurrence of rotational bands. In practice, really pure rotational bands are never realised in nuclei but instead, rotations and vibrations are more or less mixed. Even so, with a not very strict definition of a rotational band, it becomes possible to define approximately which nuclei are deformed as exemplified in fig. 11.1.

The moment of inertia $\mathscr{I}$ can be extracted from measured rotational bands. The values for deformed nuclei in the rare earth region are exhibited in fig. 11.2 together with calculated values. The experimental values are generally 25–50% of the rigid body values and can be calculated with any accuracy only when pairing correlations are introduced (appendix 14B). A simpler way to get an estimate of $\mathscr{I}$ is within the two-fluid model (see e.g. Rowe, 1970) where it is assumed that only nucleons outside the largest possible central sphere give any contribution to $\mathscr{I}$ (problem 11.1).

It was discussed in chapter 6 how the valence particle outside a spherical core determines the ground state angular momentum. This is thus a typical single-particle effect and, similarly, several valence particles may partly or fully align their angular momentum vectors to build higher spin states. Also, in deformed nuclei, similar non-collective components may be present and in this chapter we will discuss the low-energy spectra of more or less well-deformed nuclei as a mixture of single-particle and collective components where the latter are treated macroscopically. With increasing spin it becomes necessary to consider the single-particle contribution from more particles

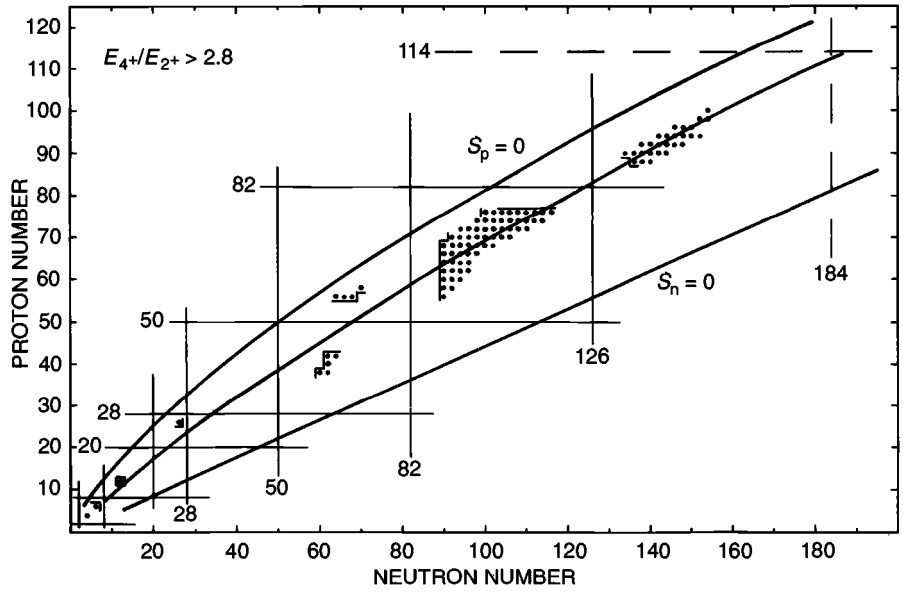

Fig. 11.1. Regions of deformed nuclei. The points represent even–even nuclei, whose excitation spectra exhibit an approximate $I(I+1)$ dependence, indicating rotational structure. An exact $I(I+1)$ dependence corresponds to $E(I=4) : E(I=2) = 3.33$. Practically all disturbances of the rotational motion will tend to decrease this value. The nuclei in the figure have been selected on the basis of the (rather arbitrary) criterion $E(I=4) : E(I=2) > 2.8$. The line of β stability and the estimated borders of instability with respect to proton and neutron emission are indicated (from Bohr and Mottelson, 1975, supplemented with data from M. Sakai, *Atomic Data and Nucl. Data Tables* **31** (1984) 399).

and at some point it seems more appropriate to consider also the collective component from a microscopic point of view. This will be discussed in chapter 12, both in the somewhat unrealistic but illustrative harmonic oscillator model and in more realistic models. In these calculations we will use the cranking model where collective and non-collective rotation are treated on the same footing. It then also becomes evident that one cannot really make a strict division between different ways to build angular momentum but that all kinds of intermediate situations occur.

11.1 Strong coupling – deformation alignment

For an odd nucleus, the specific features of the low-energy states are determined by the orbital of the odd nucleon. In chapter 8, it was found that, for such orbitals in a deformed axially symmetric potential, in addition to parity, only the projection of the angular momentum j on the symmetry axis, Ω, is

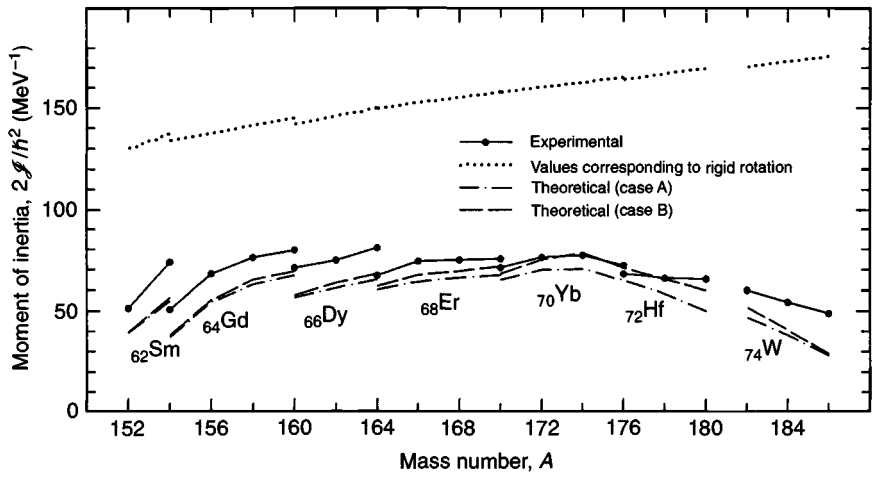

Fig. 11.2. Experimental and calculated moments of inertia of nuclei in the rare-earth region. The experimental values are extracted from the E_{2+} energies. Note that these values are far below the rigid moments of inertia. In the single-particle model with the pairing correlation correctly accounted for (dot–dashed lines), it is possible to get a fair agreement between theory and experiment. The two cases A and B correspond to somewhat different choices of the single-particle parameters (from Nilsson and Prior, 1961).

a preserved quantum number. As illustrated on the left in fig. 11.3, the total spin, **I**, is built as the sum of the spin of the odd particle, **j**, and the collective spin of the core, **R**. The core is built from all the paired nucleons. Thus, the collective energy for rotation of an axially symmetric nucleus around a perpendicular axis, the 3-axis being the symmetry axis, is calculated from

$$H_{\text{rot}} = \frac{\mathbf{R}^2}{2\mathcal{J}} = \frac{1}{2\mathcal{J}}\left[(I_1 - j_1)^2 + (I_2 - j_2)^2\right]$$
$$= \frac{1}{2\mathcal{J}}\left[\mathbf{I}^2 - I_3^2 + \left(j_1^2 + j_2^2\right) - (I_+ j_- + I_- j_+)\right]$$

The term $(I_+ j_- + I_- j_+)$ corresponds classically to the Coriolis and centrifugal forces. It gives a coupling between the motion of the particle in the deformed potential and the collective rotation. For small I it is justified to assume that this term is small and we need therefore consider only its diagonal contributions, i.e. the term $(I_+ j_- + I_- j_+)$ is treated in first order perturbation theory. This approximation, where it is assumed that the influence of the rotational motion on the intrinsic structure of the nucleus can be neglected, is generally referred to as the adiabatic approximation or the strong coupling limit. The selection rules for j_+ and j_- are $\Delta\Omega = \pm 1$. Each

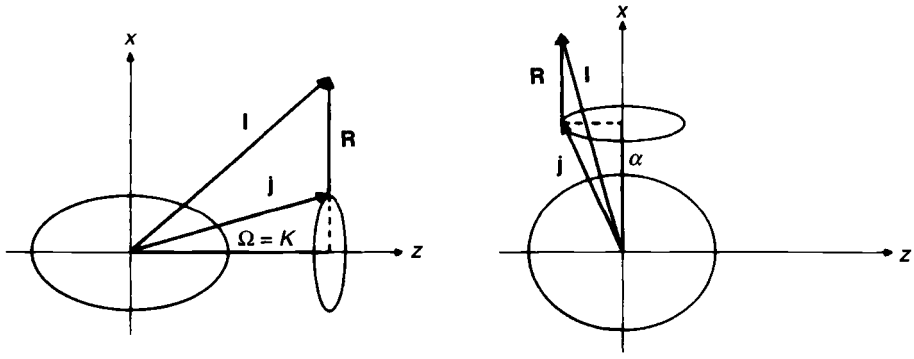

Fig. 11.3. Schematic illustration of the two extreme coupling schemes; deformation alignment (left figure) and rotation alignment (right figure) (from R.M. Lieder and H. Ryde, *Adv. in Nucl. Phys.*, eds. M. Baranger and E. Vogt (Plenum Publ. Corp., New York) vol. 10 (1978) p. 1).

orbital of the deformed potential is twice degenerate corresponding to the two possible signs of Ω. Thus, with the odd particle in one such orbital, it is only for $\Omega = \frac{1}{2}$ (or rather $\Omega = \pm\frac{1}{2}$) that the diagonal matrix elements of the $(I_+ j_- + I_- j_+)$-term are different from zero (see below).

The projection of the total angular momentum on the nuclear symmetry axis is a preserved quantum number, which is given by K, see fig. 11.3. With no collective component along this axis, $\Omega = K$. The matrix elements of $(j_1^2 + j_2^2)$, the recoil term, depend only on the particle wave function, ϕ_ν. This means that they are constant for one rotational band. We will first consider situations where they furthermore are rather small so as a first approximation, we will neglect them.

The full Hamiltonian H has the form

$$H = H_{\text{sp}} + H_{\text{rot}}$$

where H_{sp} is the deformed single-particle Hamiltonian. Its eigenvalues are the single-particle energies e_ν

$$H_{\text{sp}}\phi_\nu = e_\nu \phi_\nu$$

as exhibited in figs. 8.3 and 8.5. The total energy is now obtained as

$$E_{IK} = |e_\nu - \lambda| + \frac{\hbar^2}{2\mathscr{I}}\left[I(I+1) - K^2\right], \quad K \neq \frac{1}{2}$$

where the single-particle energy is counted relative to the Fermi level energy λ (see fig. 11.4). As $I \geq K$, the spins $I = K, K+1, K+2, \ldots$ are observed. The application of this formula may be studied in fig. 11.4. In the lower part

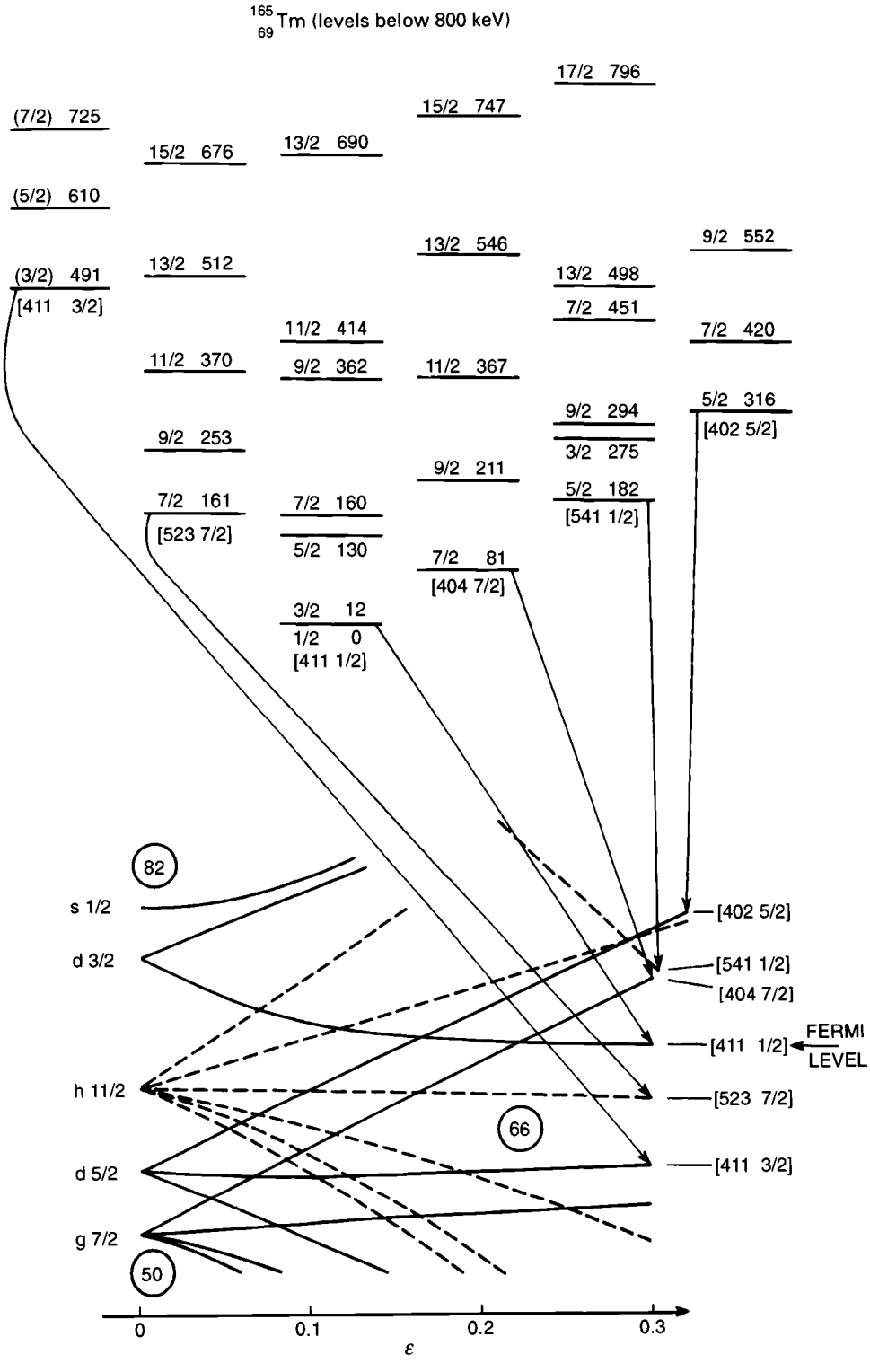

Fig. 11.4. For legend see opposite.

of this figure, the proton single-particle orbitals are exhibited as functions of the deformation coordinate, ε. For a given nucleus, the equilibrium value of ε can either be taken as an experimental quantity derivable from for example the measured quadrupole moment or it can be calculated with the methods described in chapter 9.

In the upper part of fig. 11.4, the measured low-energy spectrum of $^{165}_{69}\mathrm{Tm}_{96}$ is exhibited. For this nucleus, the equilibrium value of ε is approximately equal to 0.29. The even neutrons (96 of them) are assumed to be paired off two and two in orbitals 'Ω and $-\Omega$' to angular momentum zero. Similarly, the 68 protons are assumed to fill pairwise the 34 lowest orbitals. The 69th proton is then (for the ground state) placed in the 35th orbital, marked [411 1/2]. This is thus associated with $\Omega = \frac{1}{2}$. The ground state spin is also measured to be $\frac{1}{2}$ and a rotational band with $I = \frac{1}{2}, \frac{3}{2}, \frac{5}{2}, \ldots$ based on this orbital is identified.

At 81 keV of excitation energy there is another band starting with $I = \Omega = \frac{7}{2}$ (and having positive parity). This band is obtained by promoting the odd proton from [411 1/2] and up into [404 7/2]. The excitation energy, 81 keV, is associated with the energy difference in the single-particle diagram and described by $|e_\nu - \lambda|$ in the formula above. This energy is thus counted relative to the Fermi energy λ, where λ is given by the single-particle energy of the [411 1/2] orbital. A third band, having $K = \Omega = \frac{7}{2}$ and negative parity, is observed starting at 161 keV excitation energy. This band is realised by the promotion of one of the two protons from [523 7/2] to [411 1/2], in which latter orbital a pair state of compensating spins is formed. We may then call the $\frac{7^-}{2}$ state built on [523 7/2] a 'hole' state. From fig. 11.4, it is evident that such a hole state is associated with a positive excitation energy, thus justifying the absolute sign in the $|e_\nu - \lambda|$ term of the formula above.†

The other bands of ^{165}Tm are now easily understood. They are obtained

† If pairing is also considered, the $|e_\nu - \lambda|$ term should be replaced by a $[(e_\nu - \lambda)^2 + \Delta^2]^{1/2}$ term, see chapter 14.

Fig. 11.4. (*opposite*) Calculated single-proton orbitals in the rare-earth region with the observed spectrum of ^{165}Tm above. The usual spherical subshell notation is used for $\varepsilon = 0$. For $\varepsilon \neq 0$ the standard asymptotic notation is given for each orbital $[Nn_3\Lambda\Omega]$, N being the oscillator shell quantum number, n_3 the number of modes along the intrinsic 3-axis (the symmetry axis), Λ the value of the orbital angular momentum ℓ_3 along the 3-axis and Ω the value of the total angular momentum j_3 along the same axis. The Fermi level in the case of 69 protons is indicated. The experimental states are ordered in rotational bands and the orbital of the odd particle is indicated in each case.

simply by placing the odd proton in the orbitals indicated. The bands to the left are hole excitations, those to the right are particle excitations. A remaining problem is the $K = \frac{1}{2}$ bands, [411 1/2] and [541 1/2], which look somewhat peculiar. This is, however, what was already anticipated when it was found that the 'Coriolis term', $(I_+ j_- + I_- j_+)$, gives diagonal contributions for such bands. To calculate these contributions we will first briefly discuss the wave functions.

The orientation of a body in space is described by the three Eulerian angles α, β and γ. Two angles are needed to describe the orientation of a body-fixed axis and one to describe rotations around that axis. This means that, for a rotationally symmetric nucleus, the latter angle becomes superfluous. We will not try to derive the wave function of the collective motion but simply state that it is described by a so called $\mathscr{D}$-function, $\mathscr{D}^I_{MK}(\alpha, \beta, \gamma)$. These functions are also used to describe transformations between differently oriented coordinate systems. The quantum number M is the projection of I on the laboratory z-axis. It is a trivial quantity to which we will pay no attention subsequently. With the intrinsic wave function of the odd particle given by ϕ_ν we get the total wave function as

$$\psi_{IKM} \propto \mathscr{D}^I_{MK}(\alpha, \beta, \gamma)\, \phi_\nu(\text{intr}) = \mathscr{D}^I_{MK} \sum_{Nj} a^\nu_{N\ell j\Omega} |N\ell j\Omega\rangle$$

where in the last step we have expanded the intrinsic wave function in an $|N\ell j\Omega\rangle$-basis

$$\phi_\nu = \sum_{Nj} a^\nu_{N\ell j\Omega} |N\ell j\Omega\rangle$$

In the present discussion, we confine ourselves to nuclei having axial symmetry with respect to the 3-axis and in addition reflection symmetry with respect to a plane perpendicular to the 3-axis (these restrictions may exclude some but not very many of the nuclei that are deformed in their ground states). The nuclear shape is then mainly described by ε and ε_4 while for example $\varepsilon_3 = 0$ (cf. chapter 9). With these symmetries, there is no way to distinguish operationally between a wave function ψ_{IMK} and one $R_1\psi_{IMK}$ that is rotated 180° with respect to the 1-axis, the nuclear body-fixed x-axis. We shall therefore be required to use a new redefined wave function that is invariant with respect to the R_1-operation; $(1 + R_1)\psi$ instead of ψ. It is easy to realise that the operation with R_1 changes K to $-K$ and in addition a phase factor is introduced. The derivation of this phase factor lies outside

the scope of the present treatment so we give it without proof,

$$\psi_{IKM} \propto \sum_{Nj} a^{\nu}_{N\ell j\Omega} \left[\mathscr{D}^{I}_{MK}(\alpha,\beta,\gamma)|N\ell j\Omega\rangle + (-1)^{I-j}\mathscr{D}^{I}_{M-K}|N\ell j-\Omega\rangle \right]$$

It is now convenient to define a conjugate intrinsic state $\phi_{\bar{\nu}}$ where, however, different phase conventions are used in the literature. We will use the convention that makes the wave functions for two particles in a j-shell coupled to $I = 0$ (see chapter 14) particularly simple,

$$\phi_{\bar{\nu}} = \sum_{Nj}(-1)^{j-\Omega} a^{\nu}_{N\ell j\Omega}|N\ell j-\Omega\rangle$$

It now becomes possible to write the total wave function as

$$\psi_{IKM} \propto \left[\mathscr{D}^{I}_{MK}(\alpha,\beta,\gamma)\phi_{\nu} + (-1)^{I-K}\mathscr{D}^{I}_{M-K}(\alpha,\beta,\gamma)\phi_{\bar{\nu}} \right]$$

For $\Omega = \frac{1}{2}$, the first and the second terms of ψ_{IKM} couple through $I_+ j_-$ and $I_- j_+$. The matrix elements of $j_\pm$ are well known to be

$$\langle j\Omega|j_\pm|j\Omega \mp 1\rangle = [(j \pm \Omega)(j \mp \Omega + 1)]^{1/2}$$

When the total spin I is projected, not on the laboratory axes, but in the rotating body-fixed axes, one can show that the '+' and '–' operators change character leading to the matrix elements

$$\langle IK|I_\pm|IK \pm 1\rangle = [(I \mp K)(I \pm K + 1)]^{1/2}; \quad |IK\rangle \propto \mathscr{D}^{I}_{MK}$$

It is now straightforward to calculate the general expression for the energies of the rotational bands in the strong coupling approximation:

$$E_{IK} = E_K + \frac{\hbar^2}{2\mathscr{J}}\left[I(I+1) - K^2 + \delta_{K\frac{1}{2}} a(-1)^{I+\frac{1}{2}}\left(I+\frac{1}{2}\right)\right]$$

Here, a is the so-called decoupling parameter, which has a fixed value for each $\Omega = \frac{1}{2}$ orbital. It is calculated as

$$a = \langle\phi_{\nu}|j_+|\phi_{\bar{\nu}}\rangle = \langle\phi_{\bar{\nu}}|j_-|\phi_{\nu}\rangle = \sum_{Nj}(-1)^{j-\frac{1}{2}}\left(j+\frac{1}{2}\right)|a^{\nu}_{N\ell j\frac{1}{2}}|^2$$

where the last expression is independent of phase conventions. For an $\Omega = \frac{1}{2}$ band, the $\frac{3}{2}$ and $\frac{1}{2}$ states, the $\frac{7}{2}$ and $\frac{5}{2}$, etc. become degenerate for $a = -1$. Thus for the [411 1/2] band in fig. 11.4, a decoupling parameter $a \approx -0.8$ can be extracted. The [541 1/2] band is approximately described in the range $3 \leq a \leq 4$. However, in this case the adiabatic approximation with only one 'deformed orbital' considered and the Coriolis term, $\mathbf{I}\cdot\mathbf{j}$ treated in first order perturbation theory, is not very accurate. In the next section, we

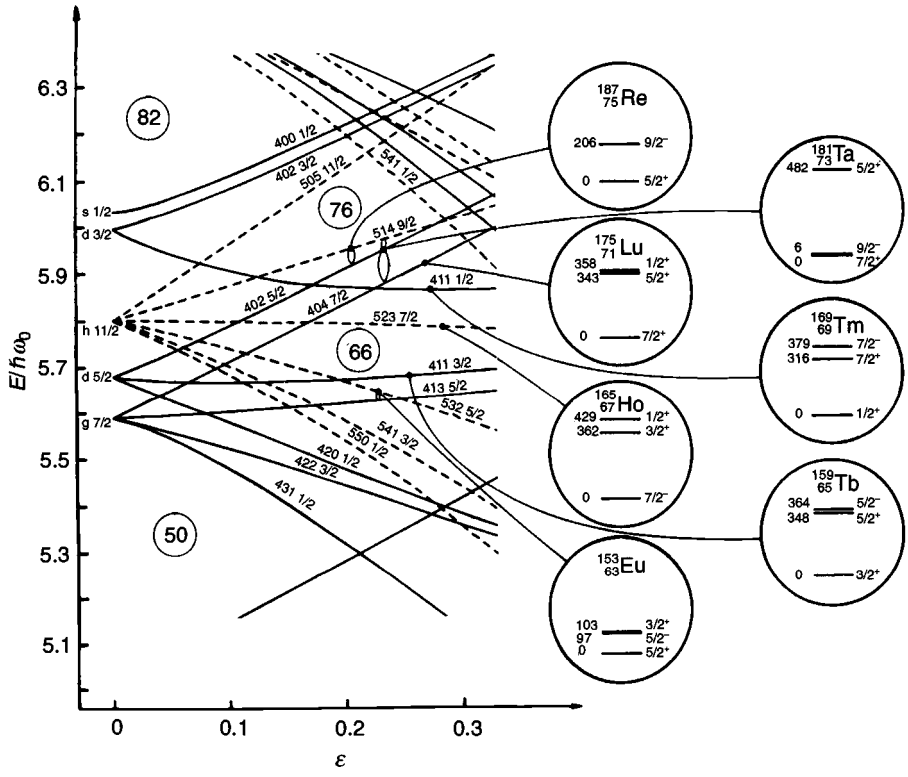

Fig. 11.5. A similar single-particle diagram as in fig. 11.4 with measured band heads of a number of odd-proton rare-earth nuclei to the right. In each case, a rotational band is built on the band heads in a similar way as for ^{165}Tm in fig. 11.4. The orbital of the ground state rotational band is indicated in each case (we are grateful to Sven Åberg who prepared this and the following figure).

will consider a different coupling scheme but, first, we will make some more comparisons between the present formalism and experimental spectra.

For a number of odd-Z nuclei with $Z = 63$–75, we show in fig. 11.5 the measured band heads together with the orbitals of the deformed shell model. On each band head, a rotational band is then built as exhibited for ^{165}Tm in fig. 11.4. The ground state ε-deformation for the nuclei in fig. 11.5 varies roughly as exhibited in the figure with ε being largest around $Z = 70$. In addition the equilibrium ε_4-value varies rather much, being negative for small Z and positive for large Z. This latter variation is not accounted for in fig. 11.5 where $\varepsilon_4 = 0$. In spite of this approximation, all the band head spins and corresponding energies come out more or less as expected from the level order in the deformed shell model.

Fig. 11.6 shows a similar comparison for odd-N nuclei with $N = 93$–107.

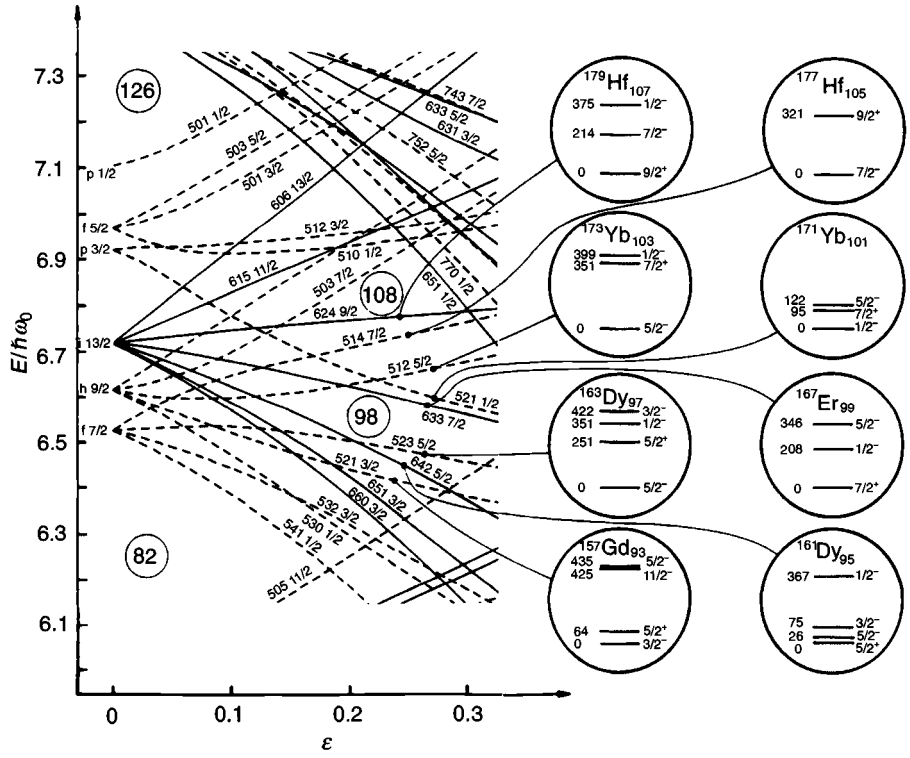

Fig. 11.6. Similar to fig. 11.5 but for neutrons instead.

Also in this case, the agreement between theory and experiment is very satisfying. In an early stage, the classification of such data as presented in figs. 11.4–11.6 played a very important role in the understanding of deformed nuclei, see e.g. Mottelson and Nilsson (1959a).

Coming back to even nuclei, we find that, for the ground state rotational band, the wave function that is properly invariant with respect to the R_1-operation takes the form

$$\psi_{I0M} \propto \mathscr{D}^I_{M0}(\alpha,\beta,\gamma)\left[1+(-1)^I\right]$$

Thus, for odd I, the wave function disappears in agreement with the fact that only even spins, $I = 0, 2, 4, \ldots$ are observed.

11.2 Decoupled bands – rotation alignment

In the preceding section, we discussed situations where the rotational motion and the nuclear deformation are essentially uncoupled. The rotational frequency was not high enough to break the coupling scheme caused by the

intrinsic deformation. The comparison with experimental spectra showed that, in many cases, this was a very reasonable approximation. However, in other cases one must expect a different coupling scheme, which is mainly determined by the rotational motion. The importance of this coupling scheme was first realised in the 1970's (Stephens, 1975).

The particle–rotor Hamiltonian can be written in the following way:

$$H = H_{\text{sp}} + H_{\text{rot}} = H_{\text{sp}} + \frac{\hbar^2}{2\mathscr{J}}\left(I^2 + j^2 - 2\mathbf{I}\cdot\mathbf{j}\right)$$

Thus, the principle of minimisation of the total energy shows that for a fixed I and for a more or less fixed j, the $\mathbf{I}\cdot\mathbf{j}$ term of the rotor Hamiltonian tries to align the intrinsic spin j with the total spin I. The latter is in most cases essentially perpendicular to the nuclear symmetry axis, the 3-axis. There will thus be a tendency towards a large perpendicular component of j contrary to the deformation aligned case (adiabatic approximation) where j is quantised along the nuclear symmetry axis (leading to $\langle j_1\rangle = \langle j_2\rangle = 0$).

The effects of the $\mathbf{I}\cdot\mathbf{j}$-term, the Coriolis term, are especially important for large j (and large I). In the rare-earth region, one notices that the high-j neutron and proton orbitals belong to the $i_{13/2}$ and $h_{11/2}$ subshells, respectively (figs. 11.5 and 11.6). These 'intruder' orbitals are uncoupled from the surrounding orbitals of different parity. In the modified oscillator potential, this is understood from the fact that they are pushed down in energy due to the ℓ^2- and $\ell\cdot\mathbf{s}$-terms. The j quantum number of these subshells is therefore almost pure up to rather large ε-values. This is in contrast to most other orbitals which are built from a mixture of several different j-values.

We will now study in some detail the neutron $i_{13/2}$ orbitals and assume that j is pure, $j = 13/2$. A quadrupole deformation along the 3-axis, $\varepsilon Y_{20}(\hat{3})$, will then split the orbitals according to

$$e_\Omega = e_0 + \frac{1}{6}\varepsilon M\omega_0^2\left\langle r^2\right\rangle \frac{3\Omega^2 - j(j+1)}{j(j+1)}$$

as was found in chapter 8 (problem 8.1). With $\left\langle r^2\right\rangle = \left(N + \frac{3}{2}\right)\hbar/M\omega_0$ where $N = 6$ and with $\hbar\omega_0 = 8$ MeV as a typical value for neutrons in the rare-earth region ($A = 160$) we get

$$e_\Omega = e_0 + 10\varepsilon\frac{3\Omega^2 - j(j+1)}{j(j+1)} \quad \text{MeV}$$

A rotational motion will try to break this coupling scheme and align the j-vector along the rotation axis instead. In the extreme case, the orbitals get

quantised along the 1-axis. We will denote the projection of j along this axis by α, see right part of fig. 11.3. Then, such a state being denoted by ϕ_α can be expressed in the ϕ_Ω states (Stephens, Diamond and Nilsson, 1973):

$$\phi_\alpha = \sum_\Omega C_\Omega \phi_\Omega$$

We will not try to evaluate the transformation coefficients, which are given by $\mathscr{D}^j_{\alpha\Omega}(0, \frac{\pi}{2}, 0)$, with $j = 13/2$ (cf. problem 11.3). In the limiting case of full alignment along the 1-axis, $\alpha = 13/2$, one would expect that mainly the small Ω-values enter and the result is

$$\left|C_{\pm 1/2}\right|^2 = 0.21, \quad \left|C_{\pm 3/2}\right|^2 = 0.16, \quad \left|C_{\pm 5/2}\right|^2 = 0.09$$

$$\left|C_{\pm 7/2}\right|^2 = 0.03, \quad \left|C_{\pm 9/2}\right|^2 = 0.01, \quad \left|C_{\pm 11/2}\right|^2 \approx \left|C_{\pm 13/2}\right|^2 \approx 0$$

The Fermi level is now placed on the $\Omega = \frac{1}{2}$ orbital and the energies of some high spin states are calculated in the two extreme coupling schemes as functions of deformation. In the deformation aligned case ($K = \Omega = \frac{1}{2}$ band), it is convenient to write the Hamiltonian as

$$H = H_{\text{sp}} + \frac{\hbar^2}{2\mathscr{J}}\left[I^2 + j^2 - 2I_3 j_3 - (I_+ j_- + I_- j_+)\right]$$

With the Fermi level on the $\Omega = \frac{1}{2}$ orbital, H_{sp} gives a zero energy contribution and we obtain

$$E = \frac{\hbar^2}{2\mathscr{J}}\left[I(I+1) + j(j+1) - 2\Omega K + a(-1)^{I+\frac{1}{2}}\left(I + \frac{1}{2}\right)\right]$$

where $j = 13/2$ and $\Omega = K = \frac{1}{2}$. In this expression, we have thus included the matrix element of $(j_1^2 + j_2^2)$, which was neglected in the preceding section. Here it is included to make the energy compatible with that calculated in the rotation aligned case below. For an orbital with pure j (and $\Omega = \frac{1}{2}$) the decoupling factor is trivially obtained as $a = (-1)^{j+\frac{1}{2}}(j + \frac{1}{2})$. Thus, in the case of $j = 13/2$, one obtains $a = -7$.

In the rotation aligned case, the energies for the $I = 13/2, 17/2, 21/2, \ldots$ states are calculated as

$$E = \sum_\Omega 2|C_\Omega|^2\left(e_\Omega - e_{\frac{1}{2}}\right) + \frac{\hbar^2}{2\mathscr{J}}\left[I(I+1) + j(j+1) - 2I\alpha\right]$$

where $j = \alpha = 13/2$ in the present case. The first term is the single-particle contribution, which gets larger the more the orbitals are spread apart, i.e. the larger the deformation becomes. This term will thus make

the rotation aligned coupling scheme disadvantageous at large deformations. The dependence of the energy splitting, $e_\Omega - e_{\frac{1}{2}}$, on ε can be calculated from the first order expression given above or can be extracted from a figure like fig. 11.6.

We also must find a value for $\hbar^2/2\mathscr{J}$. An empirical relation (Grodzins, 1962) for the rotational 2^+ energies of even nuclei is $E_{2+} \approx 1225/(A^{7/3}\beta^2)$ MeV. With β transformed to ε we get $E_{2+} \simeq 1100/(A^{7/3}\varepsilon^2)$ MeV, i.e. for $A \simeq 160$:

$$\frac{\hbar^2}{2\mathscr{J}} = \frac{E_{2+}}{6} \approx \frac{1.3}{\varepsilon^2} \quad \text{keV}$$

The two energy expressions corresponding to the deformation aligned (strongly coupled) and rotation aligned coupling schemes are compared in fig. 11.7. This figure should mainly be taken to show the trends. With increasing spin I, increasing particle spin j and decreasing deformation, the rotation aligned coupling scheme becomes more favoured. This is especially the case when the Fermi level is in the region of low-Ω orbitals of a high-j shell.

In fig. 11.7, we only plot the so-called favoured states, $I = j, j+2, j+4, \ldots$. In the pure rotation aligned case, the total nuclear wave function is symmetric with respect to an R_1-rotation and, in a similar way as for an even nucleus, the wave function for the intermediate spin states, $j+1, j+3, \ldots$ disappears. Full alignment is hardly realised in any nucleus. Experimentally, one thus often observes also the $j+1, j+3, \ldots$ states but they come relatively higher in energy than the $j, j+2, \ldots$ states.

In the rotation aligned case, the spin projection on the rotation axis, α, equals j and the rotational energy can be written

$$E_{\text{rot}} = \frac{\hbar^2}{2\mathscr{J}}[I(I+1) + j(j+1) - 2I\alpha] = \frac{\hbar^2}{2\mathscr{J}}[(I-\alpha)(I-\alpha+1) + 2\alpha]$$
$$= \frac{\hbar^2}{2\mathscr{J}}R(R+1) + \text{constant}$$

where $R = I - \alpha$ describes the collective rotation. Thus, the energy spacings in a rotation aligned spectrum of an odd nucleus should be the same as in neighbouring even nuclei. This is nicely illustrated in fig. 11.8. With 57 protons in the La nuclei, the Fermi level is situated around the [550 1/2] orbital with $j \approx 11/2$ (fig. 11.5) and rotation aligned bands starting with $I = 11/2$ are formed.

The breaking of the deformation aligned coupling scheme is generally referred to as decoupling. The wave function of the particle is then distributed

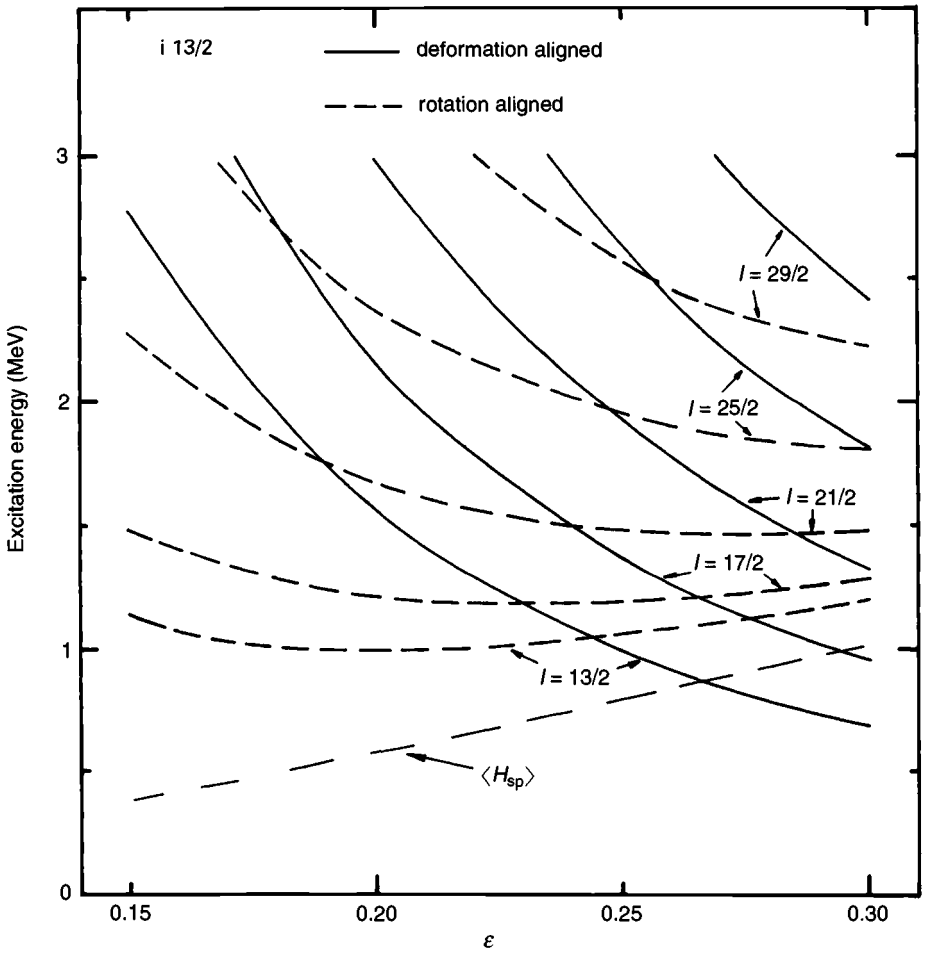

Fig. 11.7. With the Fermi level on the $\Omega = \frac{1}{2}$ state in an $i_{13/2}$ shell, the spectra of the favoured states in the two coupling schemes, deformation alignment and rotation alignment, are shown as functions of ε. The quantity $\langle H_{sp} \rangle$ is the energy required when the wave function of the odd particle is redistributed over the $i_{13/2}$ orbitals to get its spin vector aligned with the axis of rotation. One notes that small deformations and high spins tend to favour the rotation aligned scheme. If the particle–rotor Hamiltonian is fully diagonalised, a situation between the two simple models of the figure will result. However, many experimental spectra can be quite accurately described by one or the other of the two extremes.

over several 'deformed orbitals' and the spin of the particle is largely aligned along the collective rotation vector, **R**. In the idealised situation described in the present section, this alignment is complete. In the strong coupling scheme, the mixing of the $\Omega = \pm\frac{1}{2}$ orbitals correspond to a partial alignment. As the particle wave function is equally distributed over the $\Omega = \frac{1}{2}$ and the

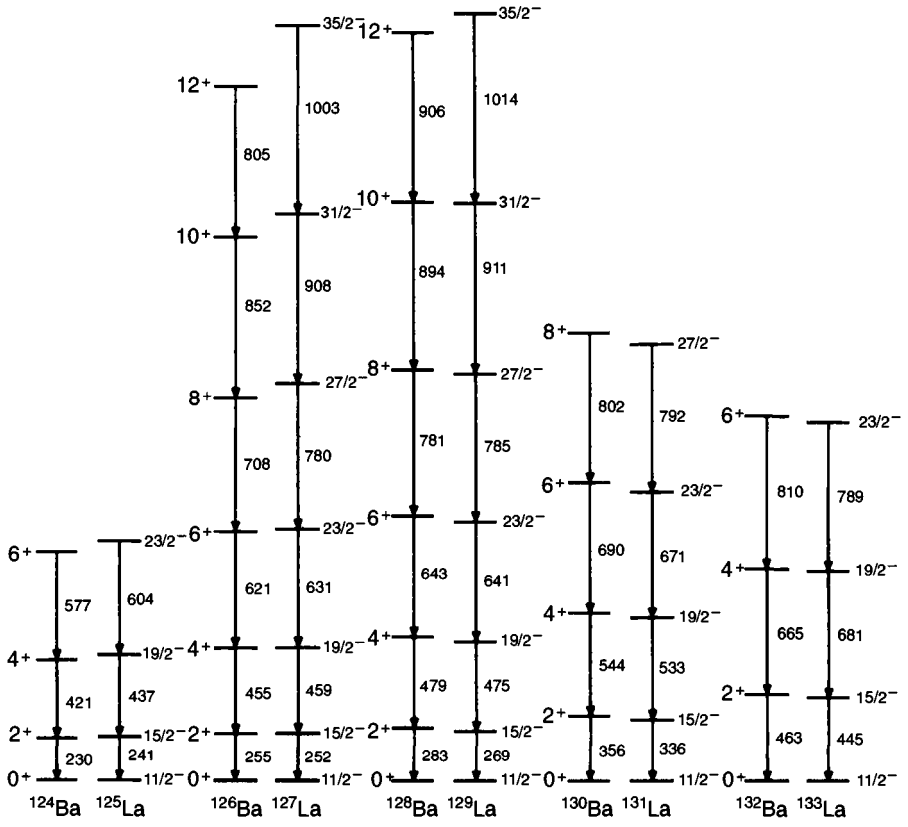

Fig. 11.8. A comparison of the rotational bands based on the $h_{11/2}$ proton orbital in the odd-mass $_{57}$La isotopes with the ground state bands of the neighbouring $_{56}$Ba nuclei. The very similar features of the neighbouring spectra suggest that the spin of the odd nuclei is obtained by simple addition of the particle spin and the collective spin, i.e. that these two spin vectors are aligned (from R.M. Lieder and H. Ryde, *Adv. Nucl. Phys.*, eds. M. Baranger and E. Vogt (Plenum Publ. Corp., New York) vol. 10 (1978) p. 1).

$\Omega = -\frac{1}{2}$ orbitals (the ν and $\bar{\nu}$ orbitals), the alignment is easily calculated as

$$\langle j_1 \rangle = \left\langle \frac{1}{\sqrt{2}} (\phi_\nu + \phi_{\bar{\nu}}) \, | j_1 | \, \frac{1}{\sqrt{2}} (\phi_\nu + \phi_{\bar{\nu}}) \right\rangle$$
$$= \frac{1}{4} \left(\langle \phi_\nu \, | j_+ | \, \phi_{\bar{\nu}} \rangle + \langle \phi_{\bar{\nu}} \, | j_- | \, \phi_\nu \rangle \right) = \frac{1}{2} a$$

For an orbital $|j\Omega\rangle = |13/2 \; 1/2\rangle$, it was found from the equation above that the decoupling factor $a = -7$, i.e. $|\langle j_1 \rangle| = 3.5$ in the strong coupling approximation. This should be compared with $\langle j_1 \rangle = \alpha = 6.5$ for full alignment in a $j = 13/2$ shell.

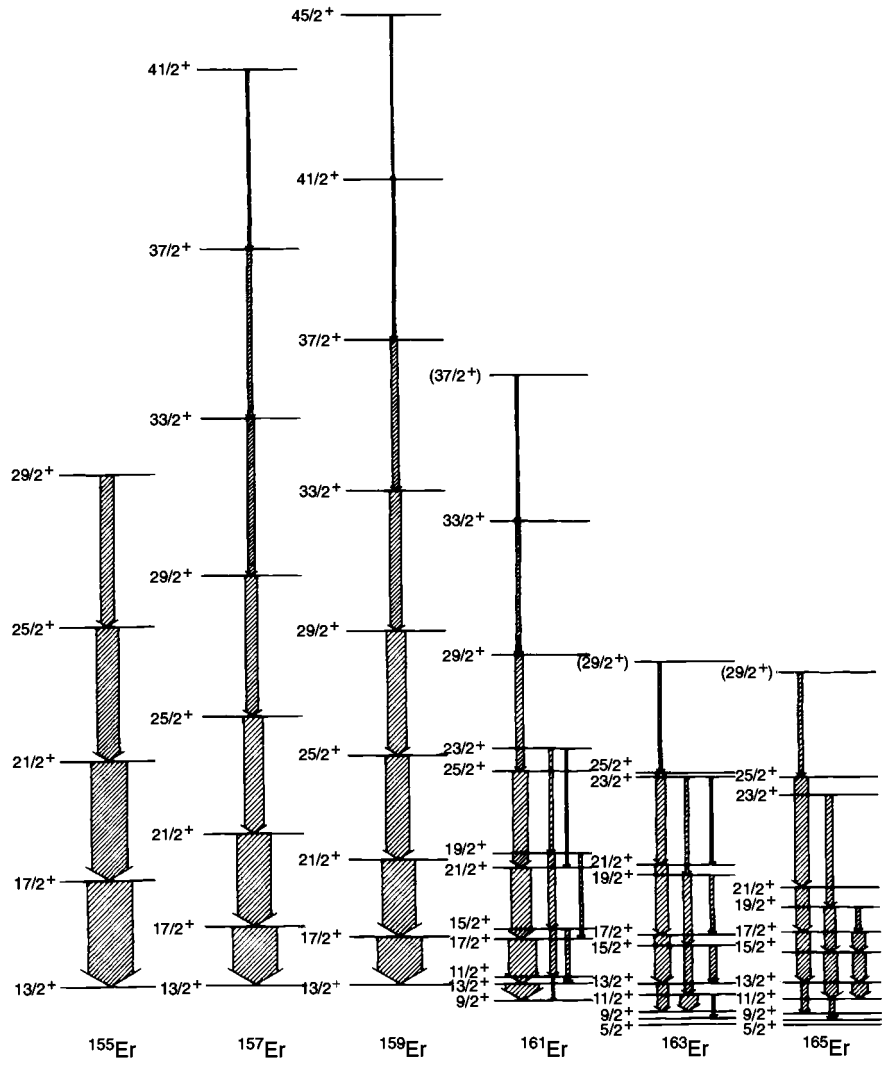

Fig. 11.9. Observed rotational bands based on the $i_{13/2}$ neutron orbitals in odd-mass $_{68}$Er isotopes. One observes a gradual change from a rotation aligned spectrum in ^{155}Er and ^{157}Er, to a deformation aligned spectrum for the lower spin states in ^{165}Er (from R.M. Lieder and H. Ryde, *Adv. Nucl. Phys.*, eds. M. Baranger and E. Vogt (Plenum Publ. Corp., New York) vol. 10 (1978) p. 1.).

The transition between the two coupling schemes is illustrated in fig. 11.9. The positive-parity spectra of the odd $_{68}$Er isotopes with $N = 89$–97 are shown. These isotopes change from being weakly deformed with the Fermi level around the $i_{13/2}$, $\Omega = \frac{1}{2}$ orbital for small N to larger deformations with the Fermi level higher up in the $i_{13/2}$ shell with increasing N. Consequently,

the spectrum is essentially decoupled for $N = 89$–91, intermediate for $N = 93$ and strongly coupled for $N = 95, 97$. Note, however, that also for these latter isotopes the high spin favoured states, $I = 17/2, 21/2, 25/2, \ldots$ come relatively lower in energy than the unfavoured $15/2, 19/2, 23/2$ states. Thus, as expected, the rotation aligned coupling scheme becomes more important with increasing spin.

Here we have only discussed the two extreme coupling schemes. It should, however, be evident that it is straightforward to diagonalise the full particle–rotor Hamiltonian and thus to describe intermediate situations as for example the spectra of ^{161}Er and ^{163}Er shown in fig. 11.9. Furthermore, only axially symmetric shapes have been considered. For the generalisation of the particle–rotor Hamiltonian to non-axial shapes, we refer to Larsson, Leander and Ragnarsson (1978) for a derivation along the lines presented here or to Meyer-ter-Vehn (1975) for a somewhat different derivation.

11.3 Two-particle excitations and back-bending

The collective angular momentum vector, **R**, is built from small contributions of all the paired nucleons. None of the wave functions is then strongly disturbed. For particles in low-Ω high-j orbitals one must, however, expect tendencies, not only for odd nucleons but also for paired nucleons, to align their spin vectors along the collective spin vector (Stephens and Simon, 1972). The maximal aligned spin for the two nucleons in a pure j-shell is then $\alpha_1 = j$ and $\alpha_2 = j - 1$, respectively, leading to a total aligned spin of $\alpha = \alpha_1 + \alpha_2 = 2j - 1$. With $R = I - \alpha$, the collective rotational energy is given by (cf. preceding section):

$$E_{\text{rot}} = \frac{\hbar^2}{2\mathscr{J}} R(R+1) = \frac{\hbar^2}{2\mathscr{J}} (I-\alpha)(I-\alpha+1)$$

The alignment is however accompanied by the breaking of one pair leading to a configuration with 'two odd particles'. A rough estimate is therefore that the energy cost for breaking the pairs is approximately twice the odd–even mass difference, 2Δ (see chapter 14). Compared to this, the energy cost for redistributing the particle wave function over the different orbitals, as discussed in the preceding section, can be neglected. Furthermore, the pairing correlations will tend to decrease this energy.

In the present approximation, we thus get for the band with 'two aligned spins'

$$E \approx 2\Delta + \frac{\hbar^2}{2\mathscr{J}} (I-\alpha)(I-\alpha+1); \quad I \geq \alpha$$

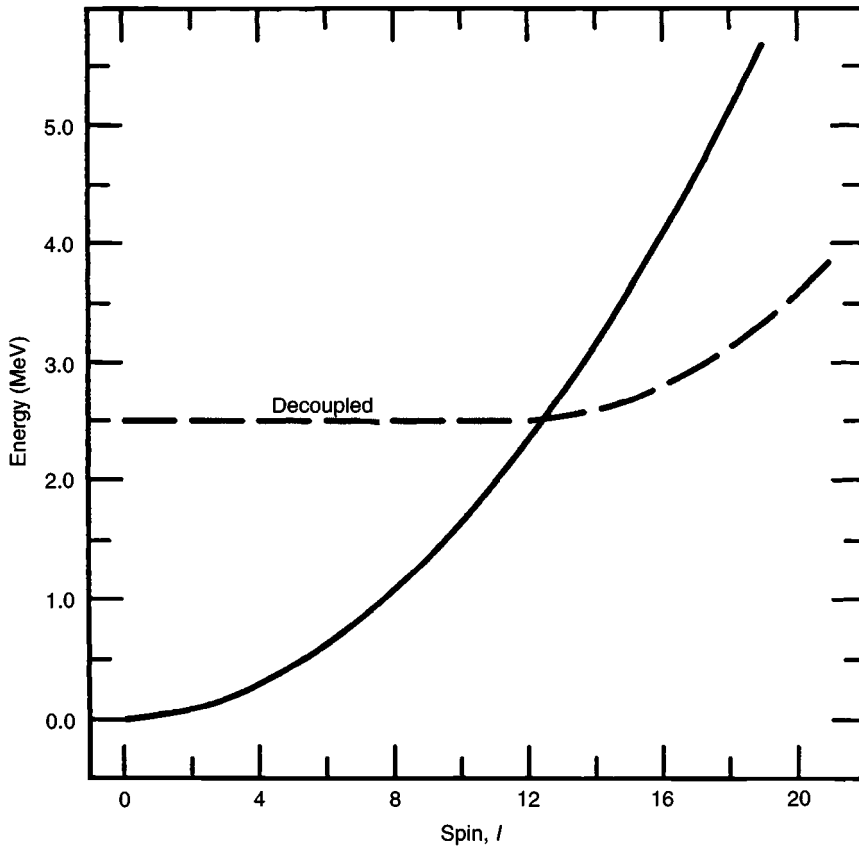

Fig. 11.10. Simple estimates are shown of the ground-band energy in an even–even $A \simeq 160$ nucleus (solid line) and the energy of a decoupled band based on two 'aligned' $i_{13/2}$ particles (dashed line) (from F.S. Stephens, *Proc. 4th Summer School on Nuclear Physics*, Rudziska, Poland, 1972, p. 190).

Total spin values smaller than the largest possible aligned spin can be obtained by a partial alignment with no collective rotation. Provided one pair is broken, this should lead to an energy $E \approx 2\Delta$. The resulting 'aligned' band is compared with the ground band in fig. 11.10.

The states having lowest possible energy for given spin are referred to as the yrast states. A typical yrast line for an $A \simeq 160$ nucleus is sketched in fig. 11.11. In this figure is also shown how the yrast levels can be studied. If two nuclei, e.g. $^{40}_{18}Ar_{22}$ and $^{124}_{52}Te_{72}$ collide in a non-central collision, a compound nucleus having a large excitation energy and a large angular momentum might be formed. By emission of e.g. four neutrons, which each carry away about 8 MeV of excitation energy (i.e. the neutron binding energy) a point some few MeV above the yrast line is reached.

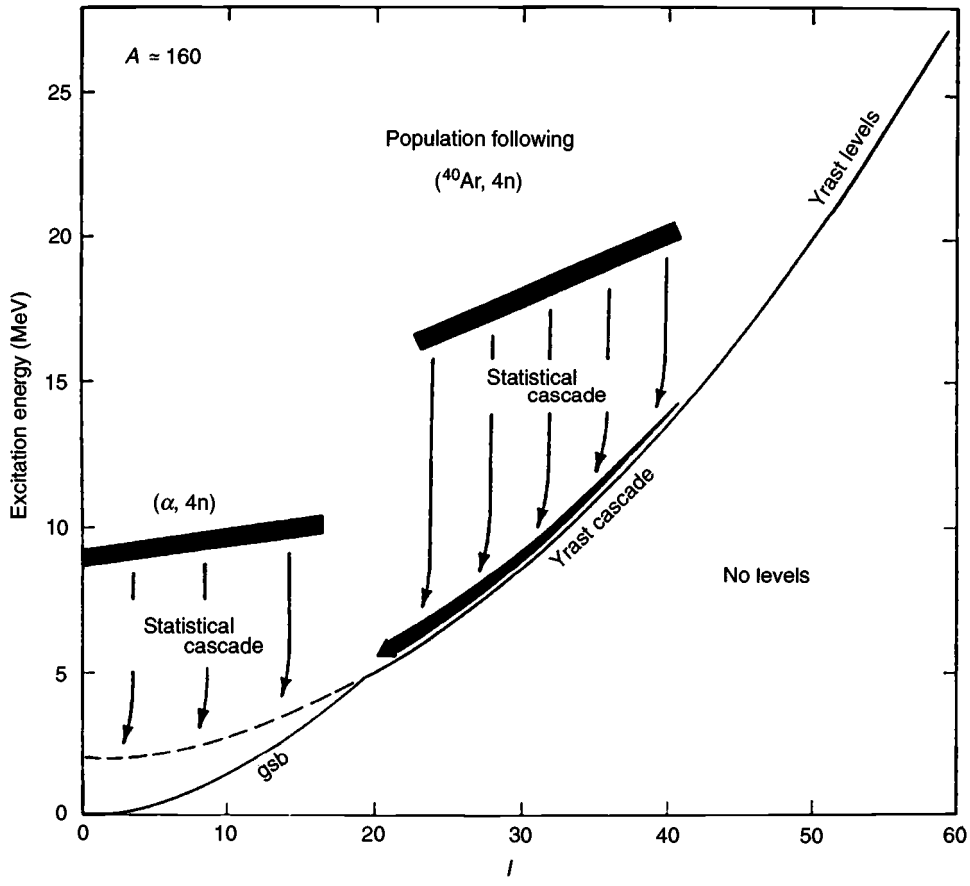

Fig. 11.11. Schematic illustration of which nuclear states are populated in reactions where either ^{40}Ar or an α-particle fuses with a target nucleus to form a compound system with $A \simeq 160$. Such reactions are best suited for the study of the yrast states, i.e. the lowest energy states for each spin I (partly from Stephens and Simon, 1972).

Some additional excitation energy might be carried away by a few so called statistical γ-rays and the yrast region is reached. The additional excitation energy is now carried by the rotational motion. For collective rotation, the compound nucleus will now de-excite mainly through E2 transitions, $(I+2) \rightarrow I$, along the yrast line. A situation like in fig. 11.10 will then lead to E2 energies that are larger for spins $I = 8$–10 than for spins $I = 14$–16.

In fig. 11.11 is also illustrated that the real high spin states can only be reached in so called heavy-ion collisions where both the projectile and the target are heavy nuclei. If an α-particle is used as projectile, only lower spin states can be reached (see problem 11.4).

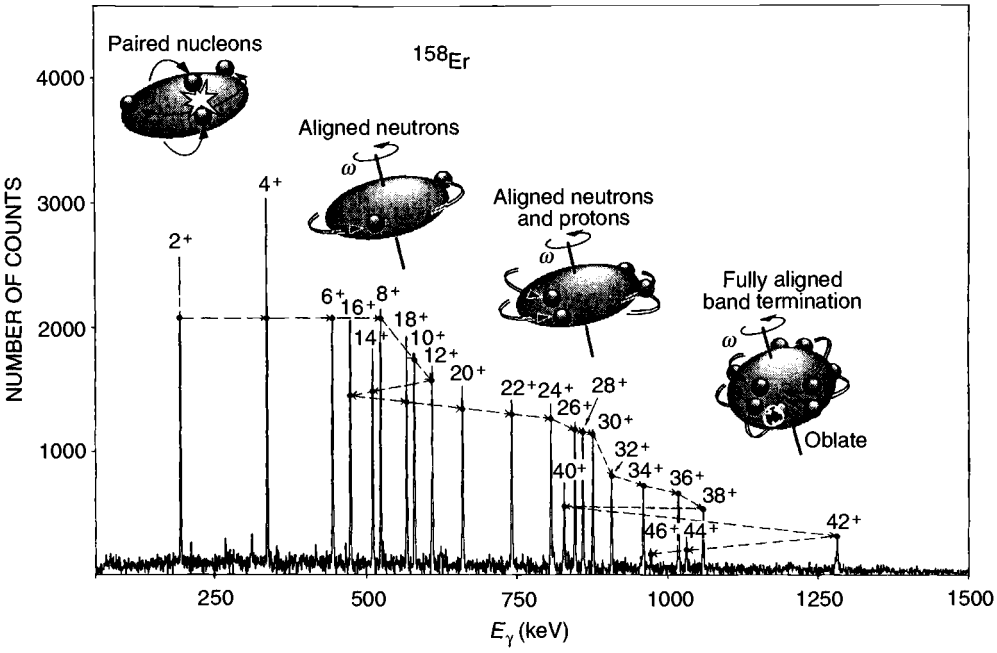

Fig. 11.12. Observed γ-ray energies of ^{158}Er formed in a reaction like the one illustrated in fig. 11.11. For $I \approx 14$ two $i_{13/2}$ neutrons become aligned resulting in a backbend while a second irregularity caused by the alignment of two $h_{11/2}$ protons is seen for $I \approx 32$. The features for $I \geq 38$ with the final band termination for $I = 46$ are discussed in chapter 12.

As seen in fig. 11.12, the experimentally observed E2 energies of ^{158}Er in the range $I = 12$–18 show the properties expected from the simple model of fig. 11.10. Of course, one must expect that the ground band and the decoupled band interact in the crossing region giving rise to a smoother transition between the two bands than shown in fig. 11.10. This is in agreement with the experimental spectrum of ^{158}Er. We must also remember that the model we have described is very much idealised. Still it seems to contain the main features of the physical effect.

The feature that the yrast E2 transition energies suddenly become smaller with increasing spin is generally referred to as back-bending (see fig. 11.12). When investigating such spectra, the yrast energies are often plotted in a somewhat different way. An effective moment of inertia as a function of the spin I can be obtained as

$$\frac{2\mathcal{J}}{\hbar^2} = \left(\frac{\mathrm{d}E}{\mathrm{d}I(I+1)}\right)^{-1} \simeq \left(\frac{E_I - E_{I-2}}{4I-2}\right)^{-1}$$

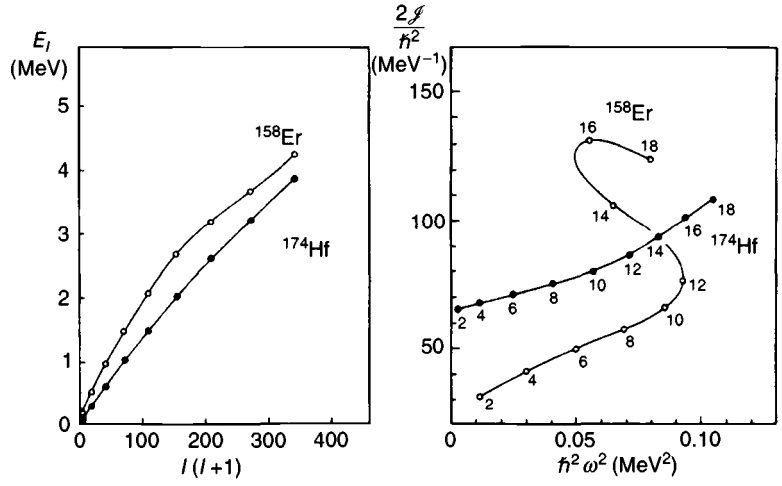

Fig. 11.13. Yrast energies in the $I = 0$–18 range of ^{158}Er and ^{174}Hf plotted versus $I(I+1)$ and corresponding back-bending plots with the moment of inertia $\mathcal{J}$ versus the squared rotational frequency, ω^2 (from R.M. Lieder and H. Ryde, *Adv. in Nucl. Phys.*, eds. M. Baranger and E. Vogt (Plenum Publ. Corp., New York) vol. 10 (1978) p. 1).

The canonical relation between the spin I and the rotational frequency ω is

$$\omega = \frac{\partial H}{\partial I}$$

Thus, in the quantum mechanical case it is natural to define

$$\hbar\omega = \frac{E_I - E_{I-2}}{[I(I+1)]^{1/2} - [(I-2)(I-1)]^{1/2}}$$

which formula is often simplified to

$$\hbar\omega = \frac{E_I - E_{I-2}}{2}$$

i.e., twice the rotational frequency is equal to the E2 transition energy.

A standard back-bending plot shows the moment of inertia $2\mathcal{J}/\hbar^2$ as a function of the squared rotational frequency. This is illustrated for ^{158}Er and ^{174}Hf in fig. 11.13. Note that while the yrast lines, E versus $I(I+1)$, look rather similar, the differences are blown up in the $\mathcal{J}$ versus ω^2 plot. Thus, ^{158}Er shows back-bending while ^{174}Hf does not.

The yrast states of ^{160}Yb and ^{164}Hf are shown in an alternative back-bending plot, I (or rather the component I_x) versus ω, in fig. 11.14. In the spin region $I = 10$–14, two $i_{13/2}$ neutrons get aligned for each nucleus. The second irregularity (up-bend) seen for ^{160}Yb at $I \approx 28$ and for ^{158}Er at

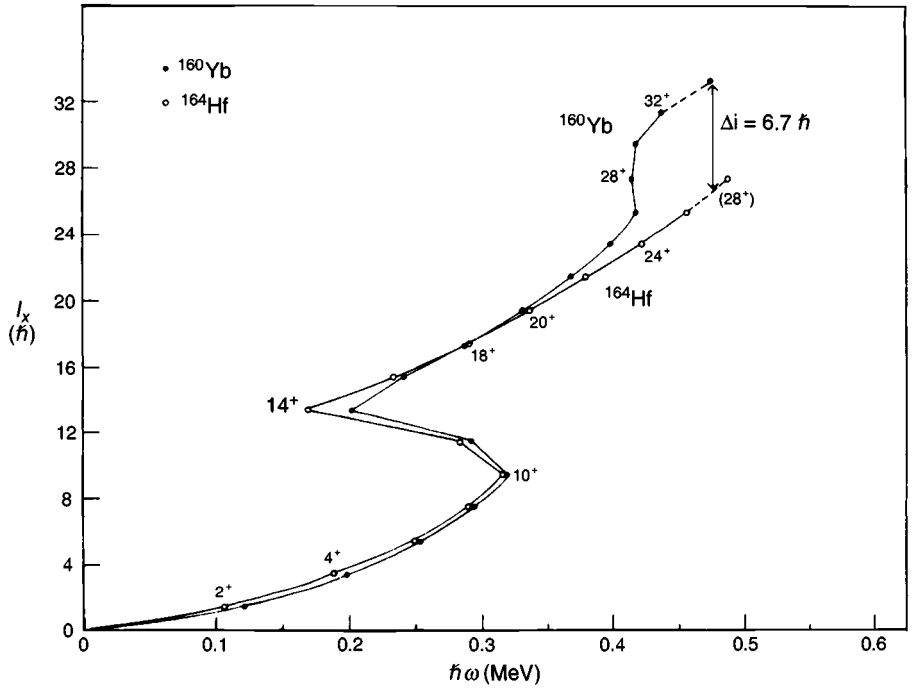

Fig. 11.14. Plot of the spin projection I_x ($\approx I$) versus $\hbar\omega$ for yrast transitions up to $I \approx 30$ in ^{160}Yb and ^{164}Hf (from L.L. Riedinger, *Phys. Scripta* **24** (1981) 312).

$I \approx 32$ (fig. 11.12) appears to be caused by alignment of two $h_{11/2}$ protons. Thus, the general features of these curves can be understood from the simple models we have discussed here. However, for any more detailed theoretical description, a proper treatment of, for example, the pairing correlations (chapter 14) becomes necessary.

Spectra of the type illustrated in figs. 11.12–11.14 have more often been described in terms of the cranking model, which is the subject of the coming chapter where, however, we concentrate on even higher spins. For more details on the description of intermediate spin states, we refer to Bengtsson and Frauendorf (1979) and Bohr and Mottelson (1977). Articles of review character have been written by for example Szymański (1983), de Voigt *et al.* (1983) and Bengtsson and Garrett (1984).

Exercises

11.1 Consider a nucleus of spheroidal shape. Calculate the moment of inertia, $\mathcal{J}$, for rigid rotation around a perpendicular axis. Compare with the value in a two-fluid model where a central sphere is assumed

to give no contribution to $\mathscr{J}$. Find the ratio of the two moments of inertia if

(a) the symmetry axis is 30% longer than the perpendicular axis ($\varepsilon = 0.25$)

(b) the symmetry axis is twice as long as the perpendicular axis ($\varepsilon = 0.6$).

11.2 The measured low-spin members of the rotational band of ^{178}Hf are given in the figure. Try to fit these values according to the rotational formula, $E_I = (\hbar^2/2\mathscr{J})I(I+1)$. Compare the resulting moment of inertia with the rigid body value. Assume spheroidal shape in calculating the latter and use the measured quadrupole moment, $Q = 7.5$ barns, as input.

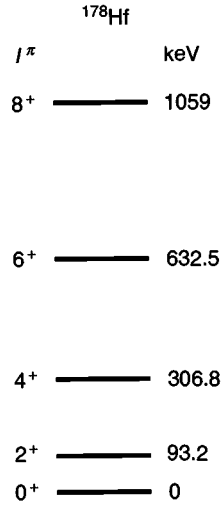

Fig. 11.15.

11.3 Find the expansion of an orbital with $j = 5/2$, $j_x = 5/2$ and $\ell = 2$ in terms of orbitals quantised along the z-axis.

11.4 Consider the situation illustrated in fig. 11.16. A nucleus with mass number A_1 is accelerated to react with another nucleus with mass number A_2. The impact parameter is equal to $(3/4)R_2$, see fig. 11.16. The aim of forming a rapidly rotating compound nucleus can only be attained if the energy of the projectile is neither too high (too high excitation energy) nor too low (the projectile will not overcome the Coulomb barrier of the target). Find the spin and the excitation

energy of the compound nucleus if the projectile, its energy and the target are

(a) ^{4}He, 60 MeV and ^{160}Dy

(b) ^{40}Ar, 180 MeV and ^{124}Sn

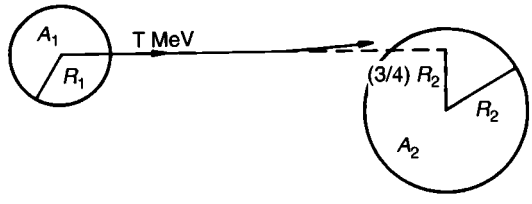

Fig. 11.16.